



Evolution of Cationic Dye Removal Via Lignocellulosic Agricultural Waste-Derived Biosorbent



Sara E. Abdelhafez,^{a*} Rehab M. Ali^{a*}

^aFabrication Technology Department, Advanced Technology and New Materials Research Institute (ATNMRI), City of Scientific Research and Technological Applications (SRTA-City), Alexandria 21934, Egypt.

Abstract

This study investigated the potential of Pyrolyzed Ficus Benjamina (PF) on the removal of cationic dye, Crystal Violet (CV), by batch biosorption processes. The consequence of contact time and temperature are examined. Characteristics of PF were investigated using Scanning Electron Microscopy (SEM), Energy-Dispersive X-ray spectroscopy (EDX), Brunauer–Emmett–Teller (BET), and Fourier Transform Infrared spectroscopy (FT-IR). The SEM analysis proved the influence of the pyrolysis process on enhancing the Ficus surface morphology by being rough and porous. The FT-IR analysis exposed the attachment of different anion functional groups, principally carboxyl, amino, and hydroxyl groups which mainly connected with the lignin chain and improved CV removal during the biosorption process. The results indicated that the biosorption efficiency of CV reached approximately 97% after 20 min of the contact time. The PF maximum biosorption capacity was 24.19 mg/g PF under the optimum conditions. The pseudo-second-order model provided the best fit to the kinetic model. The thermodynamics results revealed that CV removal using PF is a spontaneous and endothermic process. This study proved that PF is a sustainable and affordable biosorbent for CV removal from industrial outflowing.

Keywords: Ficus leaves; Crystal violet; Biosorption; Kinetics; Thermodynamic, lignocellulosic agricultural waste

1. Introduction

The accelerated industrialization expansion especially in textile production led to approximately 200 billion liters of wastewater annually. These wastes contain a significant concentration of dye (10 to 200 mg/L) which is unavoidable and affect the ecological system [1]. Textile dyes have complicated chemical structures resulting in their non-biodegradability, toxicity, and high environmental resistant forces contributing to serious problems for living organisms [2]. Cationic dyes like crystal violet, rhodamine B, malachite green, and methylene blue are the most hazardous type of dye because of their toxic, mutagenic, and carcinogenic properties as a result of their aromatic ring structure with

delocalized electrons besides their synthetic nature [3]. The (CV) dye contains the protonated amine group associated with a triphenylmethane structure [4]. As a result of the CV's high capacity to interact rapidly with other chemicals, it is commonly utilized mainly in textile dyeing besides many other industrial sectors like biological investigations, used as a mildew inhibitor in the poultry industry, pH indicator, paints, and printing ink manufacture, veterinary medicine, leather manufacturing, biological stain, and dermatological agent. The heavy usage of CV leads to discharging of high amounts of this dye in water streams which can contribute to major health issues like skin and eye damage, cancer, and kidney failure due to its

*Corresponding author e-mail: shafez@srtacity.sci.eg; (Sara E. Abdelhafez).rali@srtacity.sci.eg; (Rehab M. Ali).
EJCHEM use only; Received date 15 January 2023; revised date 24 January 2023; accepted date 27 January 2023
DOI: 10.21608/EJCHEM.2023.186831.7459

carcinogenic, poisonous, and mutagenic nature [5]. Different methods such as filtration, precipitation, coagulation, reverse osmosis, photodegradation, electrolysis, biosorption, flocculation, and oxidation have been used for the amputation of dyes from wastewater. Among these techniques, biosorption is considered one of the most popular techniques in removing pollutants from the wastewater as it does not produce by-products that pose a considerable environmental hazard, has a great depollution capacity besides its simplicity, sustainability, low cost, and effectiveness for the removal of certain pollutants, particularly dyes [6]. However, the effectiveness of the biosorption process depends greatly on the type of biosorbent, particularly, its cost, availability, synthesis procedure, efficiency, sustainability, and regeneration. Ficus Benjamina, also known as Benjamin Tree and Chinese Banyan is a genus of about 900 species of Ficus in the family Moraceae, native to Australia, south, and south-eastern Asia, then extended into the south-western Pacific, South America, southern North America, and Africa as shown in Figure 1. This tree can reach up to 20 m high in urban gardens when planted in large spaces [7]. Ficus is very popular as a result of its low price, low maintenance, attractive appearance, evergreen nature, tolerance of poor growing conditions, and its stems may be intertwined for an aesthetic view. This tree is the most common tree used in street ornamentation and this tree produces large amounts of leaf residues due to its great capacity for propagation and fast growth after pruning [7]. According to our literature search results, ficus was utilized as a reducing agent for producing several biosorbents for the removal of Malachite green (MG) [8], and metformin [9] from wastewater. However, no research article has been published on the use of ficus after only thermal treatment and without any chemical reagent for removing crystal violate.



Fig. 1: Ficus distribution around the world (with green color).

In this work, the widely available Ficus Benjamina leaves were used to produce an effective biosorbent in removing cationic dyes, Crystal Violet, after applying only applicable and affordable heat treatment. Chemical and physical characterization of pyrolyzed ficus were performed by SEM, EDX, BET and FTIR. This research focused on studying two main factors affecting the efficiency of the pollutant removal process, such as contact time and temperature. The experimental results were fitted into three kinetic modes to know which of these models gives a better correlation to experimental data. The biosorption thermodynamic data were attempted.

2. Materials and methods

2.1. Biosorbent synthesis

The used ficus leaves were selected as they should be green, as shown in Figure 2, while the yellow leaves and the leaves containing mold or rotten were excluded. To get rid of dust and impurities from the surface of the pre-selected leaves, the leaves were washed well with tap water, then filtered from the water and dried in the oven until obtain constant weight. The dried ficus leaves were ground into a fine powder to be ready for the heat treatment stage. A certain amount of ficus powder was placed in a crucible and pyrolyzed at 575°C in a muffle furnace for 3 h and labeled as PF.



Fig. 1: Sample of raw ficus leave

2.2. Preparation of dye solution

A stock solution of 1000 ppm CV ($C_{25}H_{30}N_3Cl$), MW 407.98 $g \cdot mol^{-1}$, solubility in water 16 $g \cdot L^{-1}$ at room temperature (Central drug house, New Delhi) was prepared by dissolving 0.5 g of accurately weighed dye in 500 ml of distilled water. This standard solution was diluted to prepare adjusted different concentrations, whether they were used in the calibration or the biosorption process. The dye concentration was measured in the UV spectrophotometer (Spectrophotometer 7230 G, Shanghai, China) at the wavelength of 580 nm. Four concentrations (5, 10, 15, 20 ppm) were prepared to

plot the calibration curve. The pH of the dye solution was adjusted by using 0.1 M HCl (37%, Laboratory Reagent) and 0.1 M NaOH (purity $\geq 97\%$, Sigma-Aldrich, Sweden). The chemical atom arrangement of the CV is presented in Figure 3.

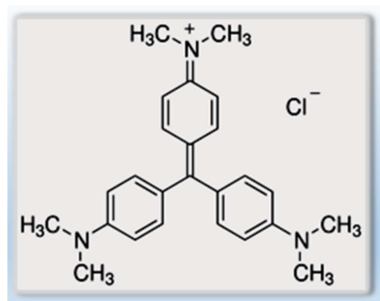


Fig. 3: Chemical atom arrangement of CV

2.3. Characterization of biosorbent

The characterizations were performed to detect the chemical and physical properties of PF biosorbent. To identify the surface morphology of the PF sample, SEM-EDX (JEOL Model JSM 6360 LA, Japan) was utilized. The PF sample was coated with a thin layer of gold palladium and a 20kV accelerating voltage was applied and the PF composition was determined from EDX analysis. The specific surface area (S_{BET}) was detected using the standard (Brunauer–Emmett–Teller) model. The whole pore volume (V_w) was estimated by altering the volume of nitrogen gas adsorbed at a relative pressure from 0.04 to 0.2 to the liquid volume of the nitrogen adsorbate at 378 K for 5h [10]. Prior to the measurements, the pre-treatment has been applied on the PF at 400 °C for 6 hr. The detected surface area and whole pore volume (V_w) were used to calculate the average pore diameter (D_p) ($D_p = 4 V_w/S_{BET}$) assuming an open-end cylindrical pore model without pore networks [2]. This study assumes that pore size less than 2 nm wide are micropores, 2–50 nm wide are mesopores, and pores with wide more than 50 nm are macropores [11]. The functional groups attached to the PF surface were identified using FTIR (Shimadzu FTIR–8400 S, Japan) in the range of 400–4000 cm^{-1} .

2.4. Batch biosorption experiments

Batch experiments were conducted to determine the effect of contact time (3-180 min), and temperature (25–65°C) on CV removal using PF. The conical flasks containing 25 ml of dye solution were in contact with the PF in an orbital shaker for a certain time at 150 rpm. The residual dye concentration was

measured after sample centrifugation at 4000 rpm for 5 min by UV spectrophotometer. Each measured absorbance was compared with the blank solution (without dye). The dye uptake and percentage removal were calculated by using Eqs. (1) and (2)

$$[12] [13] \quad q_t = \frac{(C_i - C_f)v}{m} \quad (1)$$

$$\% \text{ Removal} = \frac{C_i - C_f}{C_i} * 100 \quad (2)$$

Where q_t (mg/g) is the dye uptake at time t (min), C_i and C_f (ppm) are the initial and final concentration of CV in the solution respectively, v (L) is the volume of dye solution, and m (g) is the biosorbent weight.

2.5. Kinetic and Thermodynamic Studies

The experimental results for biosorption of 100 ppm of CV by PF at 25°C and several times (3 -180 min) were plotted in the linear forms of three different studied kinetic models 1st order, 2nd order, and intraparticle diffusion [14] [15]. The rate of the process and its mechanism were estimated from these model parameters. Moreover, the thermodynamic constants (ΔH° , ΔS° , and ΔG°) were assessed for biosorption of 100 mg. L^{-1} CV solutions and different temperature ranged from 25 to 65 °C [6]

2.6. Desorption and recycling of PF biosorbent

The evaluation of the reactivation process of the PF biosorbent is one of the most important tests that must be considered when applying the tested material at the industrial level of wastewater treatment. To identify the recyclability of PF, four different elution solutions, 0.1 M HCl, 0.1 M NaOH, and 0.1 M NaCl, were tested as regeneration solutions[10]. The PF was contaminated with CV then separated by centrifugation and dried at 60°C. Desorption was performed with a specific weight of contaminated PF with CV dye that was regenerated with 25 ml of elution solution for 30 min at 150 rpm. After desorption, The PF was separated from the eluent solution by centrifugation and dried. Afterward, fresh 25 ml of CV solution was used to test the following cycle by adding the dried regenerated PF and agitating at 150 rpm for 20 min. The biosorption-desorption cycles were studied 10 times. The optimum elution solution would be considered as the solution that recorded the highest number of PF reusability after CV biosorption processes.

3. Results and discussion

3.1. Characterization of the biosorbent

The surface morphology of the PF is detected from the SEM micrograph (Figure 4), which showed that the PF has rough layer, spherical particles and a porous surface. According to the ratio between the surface area and volume. The CV dye removal could be enhanced by the large area of these spherical particles. Further, a large volume of pores occurs, and

the biosorption efficiency and capacity increase. The EDX spectra of the studied surfaces were recorded. As shown in Figure 5, several peaks of elements (C, O, Si, Ca, and Fe) are detected in the spectrum analysis of the PF. The atomic percent existence of oxygen (54.19%), carbon (14.37%), and calcium (25.49%) significantly. The BET measurements confirmed the SEM analysis results and are represented in Figure 6. It was found that the total pore volume of PF is $3.0112 \times 10^{-2} \text{ cm}^3 \cdot \text{g}^{-1}$. Also, some volatile particles have been diffused out during heating at a high temperature which led to the development of the macropore (32.39 nm) and specific surface $3.7188 \text{ cm}^2 \cdot \text{g}^{-1}$. As it is known that the greater area exposed to the pollutant, the higher the efficiency of the biosorption process. To detect the PF surface functional groups qualitatively, FTIR spectra were subjected in the range of $4000\text{--}400 \text{ cm}^{-1}$, as shown in Figure 7. The bands in the wavelength range $3837\text{--}3738 \text{ cm}^{-1}$ are corresponding to the vibration of symmetric and asymmetric O–H group that emphasizes the presence of alcohols, phenols, and stretching vibration mode of chemisorbed and/or physisorbed water molecules in cellulose [16]– [18]. The band at 2318 cm^{-1} is corresponding to C–H symmetric and asymmetric stretching vibrations of lignocellulosic components that indicate the presence of CH₂ and/or CH₃ groups besides the –OH stretching vibrations of hydroxyl functional groups [19] [20]. The band at 1644 cm^{-1} is related to the mode of aromatic ring features [21] [22]. The existence of C=O and C=C aromatic skeletal stretching vibrations of lignin was expressed by the band at 1511 cm^{-1} [23], [24] [25]. The band at 1395 cm^{-1} represents the existence of C–O vibrations of syringyl rings of lignin [20] [26]. The bands at 1095 cm^{-1} and 1028 cm^{-1} represents the existence of C–O–C stretching β -glucosidic linkage between glucose and cellulose [27] [28]. The aryl –OH group in lignin was presented by the band at 955 cm^{-1} [29], [30]. The peak at 869 cm^{-1} is corresponding to C–OH cellulose bending [31] [20]. The functional groups of β -glycosidic bond stretch in hemicellulose and C–H bending in aromatic hydrogen at the band 754 cm^{-1} . The band at 564 cm^{-1} is related to the stretching vibration of S=O of ν_4 (SO₄²⁻) [32] [33] [3].

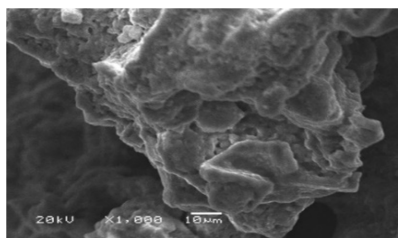


Fig. 4: SEM image of PF

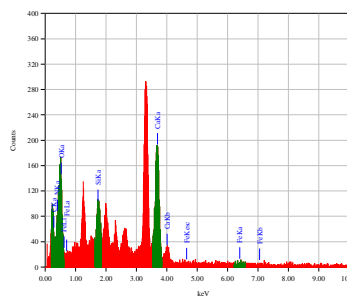


Fig. 2:EDX spectrum of PF

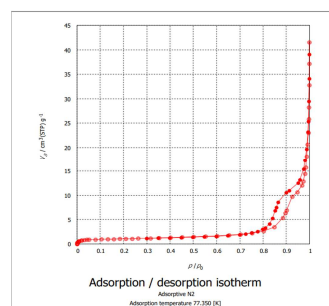


Fig. 3: BET of PF

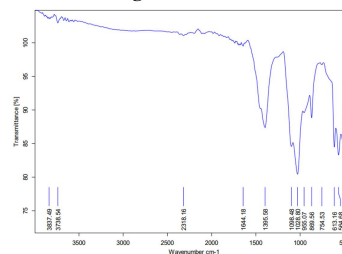


Fig. 4: FTIR spectrum of PF

3.2. The contact time effect and kinetics study

Determining the equilibrium time is one of the important factors that are studied by detecting the change in the dye concentration during the increase in the contact time between the dye and the PF biosorbent. Several aspects control the biosorption rate such as mass transfer, diffusion rate, etc. As shown in Figure 1, the biosorption process was performed in two stages. In the first 20 min, a rapid decrease in the CV concentration occurred, which indicates the ease of overcoming the resistance resulting from the liquid-solid interphase, and also the ease of convergence of the negative ions present on the PF surface and the positive ions on the CV. After 20 min, the removal rate fluctuated around the equilibrium owing to the decrease in active sites. It revealed that the strong interaction between biosorbent and dye molecules resulted in film diffusion as the main stage. Hence, it can be concluded that the biosorption of CV onto PF is quite rapid and has taken only 20 min to reach the

equilibrium. Another study used the water hyacinth to remove the CV and 40 min was recorded to reach the equilibrium [29].

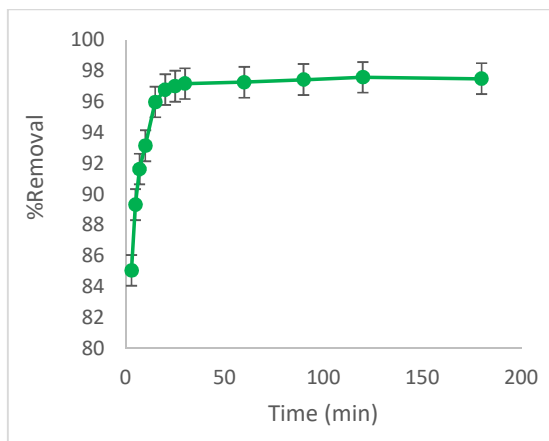


Fig. 5 The contact time effect of the CV adsorption using PF (initial concentration 100 ppm agitation speed 150 rpm, pH7.8, and adsorbent weight 0.1 g at room temperature)

A kinetic study was subjected out by applying the results of the contact time experiments in three different kinetic models. The kinetic study demonstrates the knowledge of not only the mechanism but also the rate-controlling step. As shown in Figure 2 (a), the pseudo second order model is the most compatible with the obtained result. Therefore, the chemical reaction is the main role in the CV adsorption process using PF which the exchange or sharing of electrons and valence force were induced [30]. The values of the rate constant are listed in Table 1. Wang et al. observed that the adsorption of CV onto cellulose has a similar mechanism [31]. Intra-particle diffusion model was tested to identify its involvement in the biosorption process (Figure 9 (b)). The plotted data has deviated from the origin indicated that intra-particle diffusion was not the only rate limiting step. Hence, CV biosorption onto PF is governed and limited by both, surface biosorption and intra-particle diffusion [29].

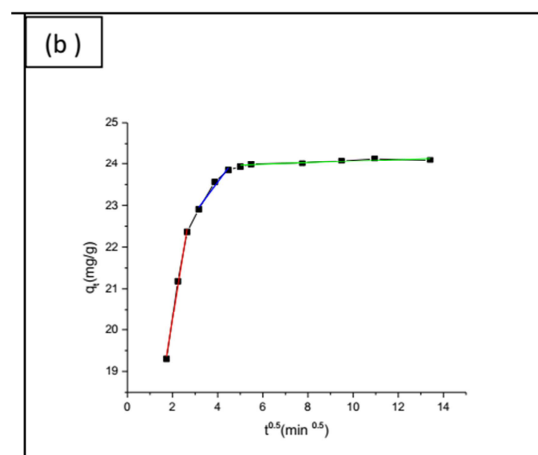
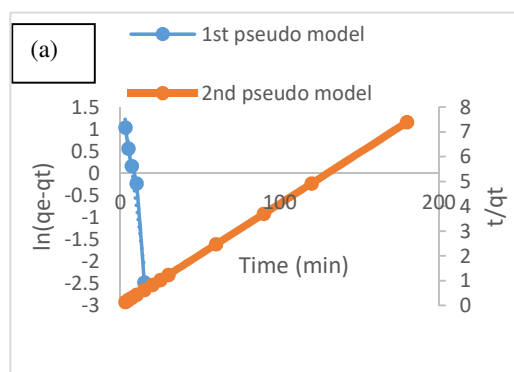


Fig. 6: The kinetic models of CV biosorption onto PF (a) Pseudo first order and Pseudo second order and (b) Intra-particle diffusion

Table 1
Kinetic parameters for the biosorption of CV on PF

$q_{e(\text{exp})}$ mg/g	24.19
Pseudo-first-order	
K_1 (min ⁻¹)	0.2819
q_e (mg/g)	7.875
R^2	0.9437
Pseudo-second-order	
K_2 (g/mg.min)	0.174
q_e (mg/g)	20.41
R^2	1
Intra-particle diffusion	
C	21.577
K_{diff} (mg/g.min ^{0.5})	0.2632
R^2	0.4314

3.3. The effect of temperature on CV uptake by PF and thermodynamic study

From the aforementioned results, it was found that PF is an efficient biosorbent for CV removal under the studied conditions. Accordingly, another important parameter was investigated for PF evaluation when adjusting its operating conditions on the industrial scale, which is the temperature. The effect of temperature on CV removal was further investigated as shown in Figure 3. When biosorption temperature increased from 25 °C to 65 °C, the %removal increased by 2.5%. That can be explained by increasing the diffusion speed of pollutant particles as a result of increasing temperature and thus the opportunity for contact between pollutant particles and the active surface of the biosorbent increases. However, the resulting improvement in the %removal

process is not worth the cost paid to adjust the temperature. Hence, the optimum biosorption temperature could be selected in this study as 25°C.

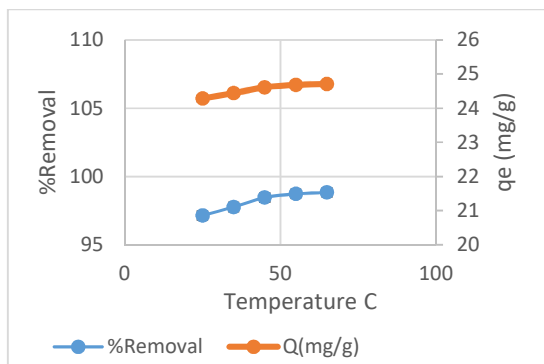


Fig. 7: The temperature effect on the CV biosorption using PF (initial concentration 100 ppm, agitation speed 150 rpm, pH 7.8, and biosorbent weight 0.1 g at room temperature).

It was also found that increasing the temperature has a positive effect on the CV biosorption process using PF. This indicates that this process is endothermic, which was eventually confirmed by the thermodynamics study. The thermodynamic parameters replicated the possibility and the spontaneity of the biosorption process. Van't Hoff equation was employed to calculate the thermodynamic parameters. The initial CV concentration was 100 ppm with different temperature ranges from 25 °C to 65°C. According to equations (3) and (4) and plotting temperature (1/T) against $\ln q_e/C_e$, the enthalpy and the entropy of the reaction were calculated from Figure 4 and listed in Table 2. The biosorption of CV onto PF was spontaneous and endothermic which was proved by the negative sign of ΔG° , and a positive sign of ΔH . It revealed that the biosorption of CV onto PF slightly increased as the temperature raised. The magnitude of ΔH suggests that the biosorption of CV onto PF was ruled by chemisorption interactions. The ΔS° positive sign is related to the change in the atomic structure of PF and the increase in randomness at the solid/liquid interphase with temperature in this biosorption process.

$$\ln \frac{q_e}{C_e} = \frac{\Delta H^\circ}{R} - \frac{\Delta S^\circ}{R} + \frac{1}{T} \quad (3)$$

$$\Delta G^\circ = \Delta H^\circ - T\Delta S^\circ \quad (4)$$

Where ΔH° is the enthalpy change (kJ/mol), ΔS° is the entropy change (kJ/mol K), ΔG° is the change in standard free energy (kJ/mol), T is the absolute temperature of biosorption (K), and R is the universal constant of gases ($8.314 \times 10^{-3} \text{ kJ K}^{-1} \text{ mol}^{-1}$).

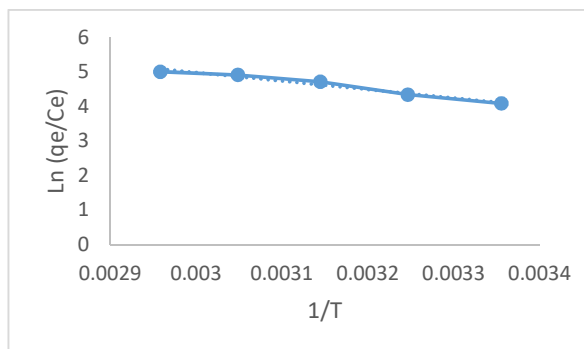


Fig. 8: Linear biosorption thermodynamic

Table 2

Thermodynamic parameters for the biosorption of CV Adsorbent onto PF

T(K)	ΔG° (kJ mol ⁻¹)	ΔH° (kJ mol ⁻¹)	ΔS° (kJ K ⁻¹ mol ⁻¹)
298	-10.1519182	20.49	0.1028
308	-11.1802772		
318	-12.2086362		
328	-13.2369952		
338	-14.2653542		
	Spontaneous	Endothermic	Randomness increase

3.4. Recyclability of PF biosorbent

To evaluate the stability and recyclability of the biosorbent, PF was regenerated and recycled for the biosorption experiments. Four solutions of HCl, H₂O, NaCl, and NaOH, were used to regenerate the PF biosorbent. It was found that HCl has a strong effect on the decomposition and dissolution of the substance, and instead, the weight used in the test vanished after the first regeneration cycle. As shown in Figure 5, generally, as the number of cycles increased, the biosorption capacity of the PF biosorbent gradually decreased, which may be due to the incomplete elution of the CV molecule during the regeneration process, and therefore resulted in a decrease in biosorption sites [32]. The H₂O showed high efficiency in reusing the PF biosorbent, as the percentage of CV removal reached 93% after the sixth cycle, while the %removal reached 90.9 and 87.2 when using NaOH and NaCl, respectively. These results proved that PF is a promising biosorbent that is relatively stable and can be easily regenerated and recycled during the CV removal process. The slight decrease in the biosorption efficiency is attributed to the incomplete desorption of CV from the PF surface. The low desorption efficiency of PF using NaOH may be due to changing the surface functional charge that is responsible for

reducing the efficiency of CV rejection. The PF biosorbent has excellent renewability and recyclability and is predictable to become an applied biosorbent for industrial wastewater treatment. Finally, the experimental data indicated that the PF offered an acceptable degree of adequate constancy and immutability for recycling and incessant removal of cationic dye from wastewater.

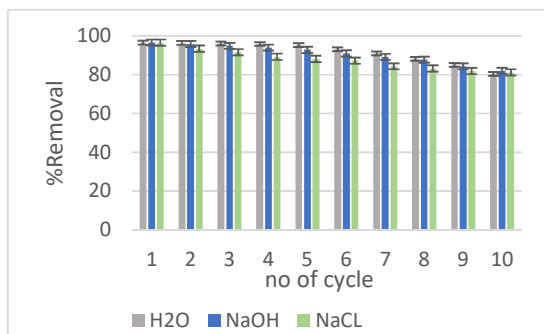


Fig. 12: Recyclability of PF biosorbent for CV removal. (initial concentration 100 ppm, biosorption time 20 min, agitation speed 150 rpm, pH 7.8, and biosorbent weight 0.1 g at room temperature)

3.5. Comparison with other studies

A comparison was studied between the previously tested biosorbents to remove the CV and the PF. As listed in the table 3, there is a convergence in the studied biosorbents results and PF, but also PF superiority by a certain quantity, which indicates that the adsorbent is a material that can remove the cationic dyes used in the textile industry. Specifically, the CV.

Table3

Compare different biosorbent on CV removal capacity

adsorbent	Q (mg/g)	ref
Pyrolyzed ficus	24	Current study
Peanut	7.9	[39]
Hazelnut	7.02	
Walnut	11.11	
Pistachio	11.31	
from tomato waste Nano-porous carbon (TWNC)	12.66	[40]
almond shell	12.2	[41]
Orange peel	19.88	[42]
rubber granulate	20.92	[43]
Sea plant leaves	22.93	[44]

4. Conclusion

pyrolyzed ficus (PF) was synthesized and utilized for CV removal from wastewater. PF has the capability to biosorb the cationic dye molecules and this could be due to the enhanced surface and

functional properties as a result of ficus pyrolysis at high temperatures. The pyrolysis process led to a rough surface and large pore size. Several characterizations were performed to detect the PF physical and chemical properties. Two important biosorption parameters, contact time and temperature, were studied to determine the rate-controlling step of the biosorption process. The maximum CV biosorption capacity was 24 mg g^{-1} , achieved at pH 7.8, contact time 20 min, using 0.1 g PF biosorbent dose, and CV initial concentration 100 ppm at room temperature. The pseudo-second-order kinetic model fitted well to the CV biosorption experimental data. The thermodynamic parameters revealed that the CV biosorption process using PF was spontaneous and endothermic in nature. The PF is recyclable and can be used in multiple biosorption cycles. In view of promising affordable biosorbents, the PF could be used as a potential biosorbent for cationic dyes biosorption from industrial effluents.

Conflicts of interest

We wish to confirm that there are no known conflicts of interest associated with this publication.

Acknowledgment

The authors also acknowledge the Central laboratory in City of Scientific Research and Technological Applications (SRTA-City) in Egypt

5. References

- [1] S. Sultana, K. Islam, M. A. Hasan, H. M. J. Khan, M. Azizur, R.Khan, A. Deb, M. Al Raihan, and M. D. W. Rahman, "Adsorption of crystal violet dye by coconut husk powder: Isotherm, kinetics and thermodynamics perspectives," *Environ. Nanotechnology, Monit. Manag.*, vol. 17, 2022, p. 100651, doi: 10.1016/j.enmm.2022.100651.
- [2] H. A. Kiwaan, F. Sh. Mohamed, A. A. El-Bindary, N. A. El-Ghamaz, H. R. Abo-Yassin, and M. A. El-Bindary, "Synthesis, identification and application of metal organic framework for removal of industrial cationic dyes," *J. Mol. Liq.*, vol. 342, 2021, p. 117435. doi: 10.1016/j.molliq.2021.117435.
- [3] R. M. Ali. E. M. El-Sayed, and H. A. Hamad, "Journey from ceramic waste to highly efficient toxic dye adsorption from aqueous solutions via one-pot synthesis of CaSO_4 rod-shape with silica," *J. Mater. Res. Technol.*, vol. 6, 2020, p. 16051–16063.

- [4] S. Shoukat, H. N. Bhatti, M. Iqbal, and S. Noreen, "Mango stone biocomposite preparation and application for crystal violet adsorption: A mechanistic study," *Microporous Mesoporous Mater.*, vol. 239, 2016, p. 180–189. doi: 10.1016/j.micromeso.2016.10.004.
- [5] Y. H. Wu, K. Xue, Q. L. Ma, T. Ma, Y. L. Ma, Y. G. Sun, and W. X. Ji, "Removal of hazardous crystal violet dye by low-cost P-type zeolite/carbon composite obtained from in situ conversion of coal gasification fine slag," *Microporous Mesoporous Mater.*, vol. 312, 2020, p. 110742. doi: 10.1016/j.micromeso.2020.110742.
- [6] H. A. Kiwaan, F. S. Mohamed, N. A. El-Ghamaz, N. M. Beshry, and A. A. El-Bindary, "Experimental and electrical studies of Na-X zeolite for the adsorption of different dyes," *J. Mol. Liq.*, vol. 332, 2021, p. 115877. doi: 10.1016/j.molliq.2021.115877.
- [7] B. G. Miao, D. R. Yang, C. Liu, Y. Q. Peng, and S. G. Compton, "The impact of a gall midge on the reproductive success of *Ficus benjamina*, a potentially invasive fig tree," *Biol. Control*, vol. 59, 2011, p. 228–233. doi: 10.1016/j.biocontrol.2011.07.007.
- [8] I. M. A. Hasan, H. M. A. Salman, and O. M. Hafez, "Ficus-mediated green synthesis of manganese oxide nanoparticles for adsorptive removal of malachite green from surface water," *Environ. Sci. Pollut. Res.*, 2022, 0123456789. doi: 10.1007/s11356-022-24199-8.
- [9] H. M. Abd El-Aziz, R. S. Farag, and S. A. Abdel-Gawad, "Removal of contaminant metformin from water by using *Ficus benjamina* zero-valent iron/copper nanoparticles," *Nanotechnol. Environ. Eng.*, vol. 5, 2020, p. 1–9. doi: 10.1007/s41204-020-00086-w.
- [10] J. H. Samat, N. N. M. Shahri, M. A. Abdullah, N. A. A. Suhaimi, K. M. Padmosoedarso, E. Kusri, A. H. Mahadi, J. Hobley and A. Usman, "Adsorption of Acid Blue 25 on Agricultural Wastes: Efficiency, Kinetics, Mechanism, and Regeneration," *Air, Soil Water Res.*, vol. 14, 2021, doi: 10.1177/11786221211057496.
- [11] T. G. Ambaye, M. Vaccari, E. D. van Hullebusch, A. Amrane, and S. Rtimi, "Mechanisms and adsorption capacities of biochar for the removal of organic and inorganic pollutants from industrial wastewater," *Int. J. Environ. Sci. Technol.*, vol. 18, 2021, p. 3273–3294. doi: 10.1007/s13762-020-03060-w.
- [12] H. A. Hamad, S. E. AbdElhafez, M. M. Elsenety, M. K. Sorour, N. K. Amin, O. Abdelwahab, E. S. Z. El-Ashtoukhy, "Fabrication and characterization of functionalized lignin-based adsorbent prepared from black liquor in the paper industry for superior removal of toxic dye," *Fuel*, vol. 323, 2022, p. 124288. doi: 10.1016/j.fuel.2022.124288.
- [13] S. E. A. Elhafez, H. A. Hamad, A. A. Zaatout, and G. F. Malash, "Management of agricultural waste for removal of heavy metals from aqueous solution: adsorption behaviors, adsorption mechanisms, environmental protection, and techno-economic analysis," *Environ. Sci. Pollut. Res.*, vol. 24, 2017, p. 1397–1415. doi: 10.1007/s11356-016-7891-7.
- [14] S. E. Abd Elhafez, A. El-Maghraby, and N. A. Taha, "Adsorption Studies of Cationic Dye on Raw And Modified Sugarcane Bagasse from Aqueous Solutions: Kinetic and Isotherm Aspects," *Egyptian Journal of Chemistry*, vol. 64, 2021, p. 1593–1600. doi: 10.21608/EJCHEM.2020.41762.2846.
- [15] R. Ali, Z. Elsagan, and S. Abdelhafez, "Lignin from Agro-Industrial Waste to an Efficient Magnetic Adsorbent for Hazardous Crystal Violet Removal," *Molecules*, vol. 27, 2022. doi: 10.3390/molecules27061831.
- [16] R. M. Ali, H. A. Hamad, M. M. Hussein, and G. F. Malash, "Potential of using green adsorbent of heavy metal removal from aqueous solutions: Adsorption kinetics, isotherm, thermodynamic, mechanism and economic analysis," *Ecol. Eng.*, vol. 91, 2016, p. 317–332. doi: 10.1016/j.ecoleng.2016.03.015.
- [17] M. A. Hassaan, M. R. Elkatory, R. M. Ali, and A. El Nemr, "Photocatalytic degradation of reactive black 5 using photo-fenton and ZnO nanoparticles under UV irradiation," *Egypt. J. Chem.*, vol. 63, 2020, p. 1443–1459. doi: 10.21608/ejchem.2019.15799.1955.
- [18] M. A. Hassaan, S. Hosny, M. R. Elkatory, R. M. Ali, T. A. Rangreez, and A. El Nemr, "Dual action of both green and chemically synthesized zinc oxide nanoparticles: Antibacterial activity and removal of congo red dye," *Desalin. Water Treat.*, vol. 218, 2021, p. 423–435. doi: 10.5004/dwt.2021.26988.
- [19] R. M. Ali, M. A. Hassaan, and M. R. Elkatory, "Towards Potential Removal of Malachite Green from Wastewater: Adsorption Process Optimization and Prediction," *Mater. Sci. Forum*, vol. 1008, 2020, p. 213–221. doi: 10.4028/www.scientific.net/msf.1008.213.
- [20] A. Hamdy, S. A. Elhafez, H. Hamad, and R. Ali, "The interplay of autoclaving with oxalate as pretreatment technique in the view of bioethanol

- production based on corn stover,” *Polymers*, vol. 13, 2021, doi: 10.3390/polym13213762.
- [21] A. Hamadi, N. Y. Mezenner, A. Lounis, R. M. Ali, and H. Hamad, “Upgrading of agro-industrial green biomass residues from chocolate industry for adsorption process: diffusion and mechanistic insights,” *J Food Sci Technol*, vol. 58, 2020, p. 081–1092.
- [22] N. TAHA, S. ABDELHAFEZ, and A. EL-MAGHRABY, “Chemical and Physical Preparation of Activated Carbon Using Raw,” *Glob. NEST Journa*, vol. 18, 2016, p. 402–415.
- [23] A. S. Elgharbawy and R. M. Ali, “Techno-economic assessment of the biodiesel production using natural minerals rocks as a heterogeneous catalyst via conventional and ultrasonic techniques,” *Renew. Energy*, vol. 191, 2022, p. 161–175. doi: 10.1016/j.renene.2022.04.020.
- [24] M. A. Hassaan, A. Pantaleo, L. Tedone, M. R. Elkatory, R. M. Ali, Ahmed El Nemr, Giuseppe De Mastro, “Enhancement of biogas production via green ZnO nanoparticles: experimental Enhancement of biogas production via green ZnO nanoparticles: experimental results of selected herbaceous crops,” *Chem. Eng. Commun.*, vol. 0, 2021, p. 1–14. doi: 10.1080/00986445.2019.1705797.
- [25] M. Elkatory et al., “Chemical mitigation technology for wax deposition in submarine oil pipeline systems,” *Egypt. J. Chem.*, vol. 64, 2021, p. 5989–5997. doi: 10.21608/ejchem.2021.72586.3604.
- [26] P. Phitsuwun, C. Permsriburasuk, S. Baramee, T. Teeravivattanakit, and K. Ratanakhanokchai, “Structural Analysis of Alkaline Pretreated Rice Straw for Ethanol Production,” *Int. J. Polym. Sci.*, vol. 2017, 2017, doi: 10.1155/2017/4876969.
- [27] S. E. AbdElhafez, T. Taha, A. E. Mansy, E. El-Desouky, M. A. Abu-Saied, K. Eltaher, A. Hamdy, G. El Fawal, A. Gamal, A. M. Hashim, A. S. Elgharbawy, M. M. Abd El-Latif, H. Hamad, and R. M. Ali, “Experimental Optimization with the Emphasis on Techno-Economic Analysis of Production and Purification of High Value-Added Bioethanol from Sustainable Corn Stover,” *Energies*, vol. 15, 2022, doi: 10.3390/en15176131.
- [28] S. Elyamny, A. Hamdy, R. Ali, and H. Hamad, “Role of Combined Na₂ HPO₄ and ZnCl₂ in the Unprecedented Catalysis of the Sequential Pretreatment of Sustainable Agricultural and Agro-Industrial Wastes in Boosting Bioethanol Production,” *Int. J. Mol. Sci.*, vol. 23, 2022, doi: 10.3390/ijms23031777.
- [29] R. M. Ali, M. R. Elkatory, H. A. Hamad, “Highly active and stable magnetically recyclable CuFe₂O₄ as a heterogenous catalyst for efficient conversion of waste frying oil to biodiesel,” *Fuel*, vol. 268, 2020, p. 117297.
- [30] D. A. Kamel, H. A. Farag, N. K. Amin, A. A. Zatout, and Rehab M. Ali, “Smart utilization of jatropha (*Jatropha curcas* Linnaeus) seeds for biodiesel production: Optimization and mechanism,” *Ind. Crop. Prod.*, vol. 111, 2018, p. 407–413.
- [31] H. Yu, W. Xiao, L. Han, and G. Huang, “Characterization of mechanical pulverization/phosphoric acid pretreatment of corn stover for enzymatic hydrolysis,” *Bioresour. Technol.*, vol. 282, 2019, p. 69–74. doi: 10.1016/j.biortech.2019.02.104.
- [32] R. M. Ali, M. M. Abd El Latif, H. A. Farag, “Preparation and Characterization of CaSO₄-SiO₂-CaO/SO₂- Composite for Biodiesel Production,” *Am. J. Appl. Chem.*, vol. 3, 2015, p. 38. doi: 10.11648/j.ajac.s.2015030301.16.
- [33] R. M. Ali, M. El Katory, M. Hassaan, K. Amer, Adel El Geiheini, “Highly Crystalline Heterogeneous Catalyst Synthesis from Industrial Waste for Sustainable Biodiesel Production,” *Egypt. J. Chem*, vol. 63, 2020, p. 1161–1178.
- [34] M. R. Kulkarni, T. Revanth, A. Acharya, and P. Bhat, “Removal of Crystal Violet dye from aqueous solution using water hyacinth: Equilibrium, kinetics and thermodynamics study,” *Resour. Technol.*, vol. 3, 2017, p. 71–77. doi: 10.1016/j.refit.2017.01.009.
- [35] H. Wei, J. Sun, B. Zhang, and R. Liu, “Comparative Study of Cationic Dye Adsorption Using Industrial Latex Sludge with Sulfonate and Pyrolysis Treatment,” *Sustainability*, vol. 12, 2020, 10048; doi:10.3390/su122310048
- [36] S. Wang, W. Chen, C. Zhang, and H. Pan, “Efficient and selective adsorption of cationic dyes with regenerated cellulose,” *Chem. Phys. Lett.*, vol. 784, 2021, p. 139104. doi: 10.1016/j.cplett.2021.139104.
- [37] H. Fakhry, M. El-Sonbati, B. Omar, R. El-Henawy, Y. Zhang, and M. EL-Kady, “Novel fabricated low-cost hybrid polyacrylonitrile/polyvinylpyrrolidone coated polyurethane foam (PAN/PVP@PUF) membrane for the decolorization of cationic and anionic dyes,” *J. Environ. Manage.*, vol. 315, 2022, doi: 10.1016/j.jenvman.2022.115128.
- [38] C. Huang, B. Cai, L. Zhang, C. Zhang, and H. Pan, “Preparation of iron-based metal-organic framework @cellulose aerogel by in situ growth method and its application to dye adsorption,” *J.*

- Solid State Chem., vol. 297, 2021, p. 122030, doi: 10.1016/j.jssc.2021.122030.
- [39] M. Saleh, Z. Isik, E. Yabalak, M. Yalvac, and N. Dizge, "Green production of hydrochar nut group from waste materials in subcritical water medium and investigation of their adsorption performance for crystal violet," *Water Environ. Res.*, vol. 93, 2021, p. 3075–3089. doi: 10.1002/wer.1659.
- [40] F. Guzel, H. Saygili, G. I. A. Saygili, iliz Koyuncu a "Decolorisation of aqueous crystal violet solution by a new nanoporous carbon : Equilibrium and kinetic approach," *Journal of Industrial and Engineering Chemistry, Decolorisation of aqueous crystal violet solution by a new nanoporous carbon : Equilibrium and ,* 2014, doi: 10.1016/j.jiec.2013.12.023.
- [41] I. Loulidi, F. Boukhlifi, M. Ouchabi, A. Amar, M. Jabri, A. Kali, S. Chraibi, C. Hadey, and F. Aziz, "Adsorption of Crystal Violet onto an Agricultural Waste Residue : Kinetics , Isotherm , Thermodynamics , and Mechanism of Adsorption," vol. 2020, 2020, <https://doi.org/10.1155/2020/5873521>
- [42] R. Sivaraj, C. Namasivayam, and K. Kadirvelu, "Orange peel as an adsorbent in the removal of Acid violet 17 (acid dye) from aqueous solutions," *Waste Manag.*, vol. 21, 2001, p. 105–110. doi: 10.1016/S0956-053X(00)00076-3.
- [43] M. Sulyman, J. Kucinska-lipka, and M. Sienkiewicz, "Development , characterization and evaluation of composite adsorbent for the adsorption of crystal violet from aqueous solution: Isotherm , kinetics , and thermodynamic studies," *Arab. J. Chem.*, vol. 14, 2021, p. 103115. doi: 10.1016/j.arabjc.2021.103115.
- [44] P. P. Kyi, J. O. Quansah, C. Lee, and J. Moon, "applied sciences The Removal of Crystal Violet from Textile," *Appl. Sci.*, vol. 10, 2020, 2251. <https://doi.org/10.3390/app10072251>